

Interaction between Protein Kinase C μ and the Vanilloid Receptor Type 1*

Received for publication, September 8, 2004
Published, JBC Papers in Press, October 7, 2004, DOI 10.1074/jbc.M410331200

Yun Wang \ddagger §¶, Noemi Kedei \ddagger , Min Wang \S , Q. Jane Wang \ddagger ||, Anna R. Huppler \ddagger , Attila Toth \ddagger ,
Richard Tran \ddagger , and Peter M. Blumberg \ddagger **

From \ddagger NCI, National Institutes of Health, Bethesda, Maryland 20892-4255 and the \S Neuroscience Research Institute, Peking University, Beijing 100083, China

The capsaicin receptor VR1 is a polymodal nociceptor activated by multiple stimuli. It has been reported that protein kinase C plays a role in the sensitization of VR1. Protein kinase D/PKC μ is a member of the protein kinase D serine/threonine kinase family that exhibits structural, enzymological, and regulatory features distinct from those of the PKCs, with which they are related. As part of our effort to optimize conditions for evaluating VR1 pharmacology, we found that treatment of Chinese hamster ovary (CHO) cells heterologously expressing rat VR1 (CHO/rVR1) with butyrate enhanced rVR1 expression and activity. The expression of PKC μ and PKC β 1, but not of other PKC isoforms, was also enhanced by butyrate treatment, suggesting the possibility that these two isoforms might contribute to the enhanced activity of rVR1. In support of this hypothesis, we found the following. 1) Overexpression of PKC μ enhanced the response of rVR1 to capsaicin and low pH, and expression of a dominant negative variant of PKC μ reduced the response of rVR1. 2) Reduction of endogenous PKC μ using antisense oligonucleotides decreased the response of exogenous rVR1 expressed in CHO cells as well as of endogenous rVR1 in dorsal root ganglion neurons. 3) PKC μ localized to the plasma membrane when overexpressed in CHO/rVR1 cells. 4) PKC μ directly bound to rVR1 expressed in CHO cells as well as to endogenous rVR1 in dorsal root ganglia or to an N-terminal fragment of rVR1, indicating a direct interaction between PKC μ and rVR1. 5) PKC μ directly phosphorylated rVR1 or a longer N-terminal fragment (amino acids 1–118) of rVR1 but not a shorter one (amino acids 1–99). 6) Mutation of S116A in rVR1 blocked both the phosphorylation of rVR1 by PKC μ and the enhancement by PKC μ of the rVR1 response to capsaicin. We conclude that PKC μ functions as a direct modulator of rVR1.

The vanilloid receptor type 1 (VR1 or TRPV1)¹ is a vanilloid-gated, nonselective cation channel that belongs to the transient receptor potential (TRP) channel superfamily. VR1 is expressed on small diameter neurons within sensory ganglia and accounts for the highly selective action of vanilloids as excitatory agents for nociceptors. In addition to vanilloids, heat and protons also influence vanilloid receptors and nociceptive pathways, and VR1 thus can be viewed as a molecular integrator of chemical and physical stimuli that elicit pain (1). Following tissue injury, the magnitude of VR1 responses is modulated by the combined effects of protons, temperature, endogenous ligands, and signaling pathways, and this modulation of VR1 activity contributes to the sensitization of nociceptors associated with the development of allodynia and hyperalgesia (2).

Current evidence implicates multiple signaling pathways in the modulation of VR1. PKA reduces vanilloid receptor type 1 (VR1) desensitization and directly phosphorylates VR1 (3). PKC α contributes to VR1 activation by pH (4), and PKC ϵ both directly phosphorylates VR1 and is implicated in the development of hyperalgesia (19). Finally, p38 mitogen-activated protein kinase activation increases the level of VR1 and maintains hyperalgesia to heat (5).

PKD/PKC μ , PKD3/PKC ν , and PKD2 represent a class of diacylglycerol-responsive protein kinases related to but distinct from the PKCs. Features distinguishing the PKD/PKC μ family members from the PKCs include a catalytic domain that is distantly related to the calmodulin kinase domain while showing little similarity to the highly conserved PKC catalytic domain, the presence of a pleckstrin homology domain, the lack of a pseudosubstrate domain, and the lack of a C2 domain. In addition, the tandem C1 domains, which account for the recognition of diacylglycerol and the phorbol esters, are more widely separated than in the PKCs (6).

The regulation of PKD/PKC μ is distinct from that of the PKCs. In the case of the PKCs, binding of diacylglycerol/phorbol ester to the C1 domain induces a conformational change in the enzyme, removing the pseudosubstrate inhibitory region from the catalytic site and thereby activating the enzyme. In addition, by completing the hydrophobic surface on the C1 domain, the bound diacylglycerol/phorbol ester drives the membrane association of the PKC. The localization of the PKC,

* This work was supported in part by a grant from the National Natural Science Foundation of China (30330026) (to J. S. Han), by a National Basic Research Program of China Grant (G1999054000) (to Y. W.), and by an Outstanding Young Teacher of Higher Academic School Grant 2001-182 (to Y. W.) from the Ministry of Education of China. The costs of publication of this article were defrayed in part by the payment of page charges. This article must therefore be hereby marked "advertisement" in accordance with 18 U.S.C. Section 1734 solely to indicate this fact.

¶ To whom correspondence may be addressed: Neuroscience Research Institute, Dept. of Neurobiology, Peking University, 38 Xue Yuan Rd., Beijing 100083, China. Tel.: 86-10-828201119; Fax: 86-10-82801111; E-mail: wangy66@bjmu.edu.cn.

|| Present address: Dept. of Pharmacology, University of Pittsburgh, Pittsburgh, PA 15261.

** To whom correspondence may be addressed: National Cancer Institute, Bldg. 37, Rm. 4048, 37 Convent Dr., MSC 4255, Bethesda, MD 20892-4255. Tel.: 301-496-3189; Fax: 301-496-8709; E-mail: blumberp@dc37a.nci.nih.gov.

¹ The abbreviations used are: VR1, vanilloid receptor type 1; TRP, transient receptor potential; rVR1, cloned rat vanilloid receptor subtype 1; CHO, Chinese hamster ovary; CHO/rVR1 cell, Chinese hamster ovary cells transfected with rVR1; PKC, protein kinase C; PKD, protein kinase D; DRG, dorsal root ganglion; DMEM, Dulbecco's modified Eagle's medium; DPBS, Dulbecco's modified PBS; GFP, green fluorescent protein; GST, glutathione S-transferase; PMA, phorbol 12-myristate 13-acetate; PBS, phosphate-buffered saline; MES, 4-morpholinethanesulfonic acid; TBS, Tris-buffered saline; Tricine, N-[2-hydroxy-1,1-bis(hydroxymethyl)ethyl]glycine.

in turn, determines which of its possible substrates are accessible for phosphorylation. In the case of PKD/PKC μ , the diacylglycerol/phorbol ester has two distinct effects. First, the diacylglycerol/phorbol ester activates the PKCs, which phosphorylate PKD/PKC μ and lead to its activation. This state of activation of phosphorylated PKD is maintained during cell disruption and immunoprecipitation, whereas for PKCs, their *in vitro* activity remains dependent on the presence of lipid cofactors (7). Second, by binding to the C1 domains of PKD/PKC μ , the diacylglycerol/phorbol ester drives the membrane association of the PKD/PKC μ (8).

Selective protein-protein interactions and phosphorylation of unique downstream effectors are likely to form the basis of isotype-specific functions. Each PKC family member shows an optimal substrate consensus sequence. PKD/PKC μ , in particular, has substrate specificity very different from PKC isoforms. These substrates include phosphatidylinositol kinases (9), 14-3-3 proteins (10), the B-cell receptor complex (11), the tyrosine kinase Syk (12), phospholipase C γ 1 (11), Btk (Bruton's tyrosine kinase) (8), and a novel neuronal substrate of protein kinase D, Kidins220 (kinase D-interacting substrate of 220 kDa) (13).

As part of our effort to optimize conditions for evaluating VR1 pharmacology, we found that treatment with butyrate of Chinese hamster ovary (CHO) cells heterologously expressing VR1 (CHO/rVR1) enhanced rVR1 expression and activity. Butyrate is known to function as an inhibitor of histone deacetylase and affects the transcription of some genes. We found that the expression of PKC μ and PKC β 1, but not other PKC isoforms, was also enhanced by butyrate treatment, raising the possibility that these two isoforms might contribute to the enhanced activity of rVR1. In support of this hypothesis, we found that PKC μ directly bound to and phosphorylated rVR1. Overexpression of PKC μ enhanced rVR1 activity, and reduced expression of PKC μ by means of antisense oligonucleotides or inhibition of its function through a dominant negative mutant of PKC μ reduced rVR1 activity. We conclude that PKC μ functions as a direct modulator of VR1.

EXPERIMENTAL PROCEDURES

Materials—[γ -³³P]ATP (5000 Ci/mmol, 37 GBq = 1 mCi) was obtained from ICN (Irvine, CA), and phorbol 12-myristate 13-acetate (PMA) was from LC Laboratories (Woburn, MA). Anti-capsaicin receptor antibody was from Calbiochem. PKC μ (C-20) and PKC β 1 antibodies were from Santa Cruz Biotechnology, Inc. (Santa Cruz, CA). Green fluorescent protein (GFP) antibody was from Roche Applied Science. GST antibody was from Amersham Biosciences. Cell culture reagents and Lipofectamine were obtained from Invitrogen.

Preparation and Subculture of Cells Stably Expressing Rat VR1—CHO cells stably transfected with rat VR1 in a pTet off regulatory system were described previously (14). In this system, expression of the rVR1 is repressed in the presence of tetracycline (1 μ g/ml) but is induced upon removal of the antibiotic (14). For radioligand binding experiments, cells were seeded in T75 cell culture flasks in the culture medium with tetracycline (1 μ g/ml) and Geneticin (0.25 mg/ml). After 2 days, the culture medium was changed to medium without tetracycline, and the cells were grown for an additional 48 h to induce rVR1 expression. The flasks were washed with PBS, and the cells were harvested in PBS containing 5 mM EDTA. The cells were pelleted by gentle centrifugation and stored at -20°C until assayed. For assay of ⁴⁵Ca²⁺ uptake, cells were seeded into 24-well plates in medium with tetracycline (1 μ g/ml) and Geneticin (0.25 mg/ml). After 1 day, the culture medium was changed to medium without tetracycline, and the cells were grown for an additional 48 h to induce rVR1 expression. For calcium imaging, cells were grown on round glass coverslips (25 mm).

DRG Neuron Isolation and Culture—2–3-Week-old male Sprague-Dawley rats were provided by the Institute of Animal Research of the Chinese Academy of Sciences. The experimental protocols were approved by the Animal Care and Use Committee of Peking University Health Science Center. Rats were killed by decapitation under CO₂ anesthesia. The spinal columns were removed aseptically, and dorsal root ganglia from all levels were dissected out and collected in DMEM containing 0.5% heat-inactivated fetal bovine serum (Invitrogen), 1 mM

sodium pyruvate, 25 mM HEPES, and penicillin/streptomycin (Invitrogen). Ganglia were digested with 1 mg/ml collagenase (Sigma) and 0.125 mg/ml trypsin (Sigma) for 30 min at 37 $^{\circ}\text{C}$. Then fetal bovine serum was added to terminate the digestion. The ganglia were triturated through a flame-polished Pasteur pipette to form a single cell suspension. Cells were then washed three times with DMEM and resuspended in the same medium, and the number of viable cells was determined. Cells were plated in 10 μ g/ml polylysine-coated coverslips and treated with 10⁻⁵ M cytosine arabinoside (Sigma) for 24 h. They were then cultured for 2 days in DMEM containing 10% fetal bovine serum, penicillin/streptomycin, and 200 ng/ml mouse submaxillary gland 2.5S nerve growth factor (Sigma) before being used for experiments.

⁴⁵Ca²⁺ Uptake—CHO/rVR1 cells or DRG neurons were incubated for 5 min at 37 $^{\circ}\text{C}$ in DMEM without serum, 0.25 mg/ml bovine serum albumin, 0.2 μ Ci/well ⁴⁵Ca²⁺, and capsaicin as indicated. To determine the heat dependence of ⁴⁵Ca²⁺ uptake, cells were incubated for 5 min at 44 $^{\circ}\text{C}$ in the medium specified above. To determine the pH dependence of ⁴⁵Ca²⁺ uptake, cells were incubated for 5 min at 37 $^{\circ}\text{C}$ in the presence of Dulbecco's modified PBS with Ca²⁺ and Mg²⁺ (DPBS) supplemented with 0.25 mg/ml bovine serum albumin, 0.2 μ Ci/well ⁴⁵Ca²⁺, and various concentrations of the different compounds, adjusted to the indicated pH with 1 M MES (Sigma). After incubation, cells were washed three times with DPBS (with Ca²⁺ and Mg²⁺) and lysed in 400 μ l/well radioimmune precipitation assay buffer (50 mM Tris-HCl, pH 7.5, 150 mM NaCl, 1% Triton X-100, 1% deoxycholate, 0.1% SDS) for 20 min. Aliquots of the solubilized cell extracts were counted in a liquid scintillation counter.

Imaging of Intracellular Calcium Levels ([Ca²⁺]_i)—CHO/rVR1 cells or DRG neurons grown on coverslips were loaded with Fura-2/AM (10 μ M) (Molecular Probes, Inc., Eugene, OR) for 10 min at 37 $^{\circ}\text{C}$ and an additional 50 min at room temperature (for CHO/rVR1 cells), washed, and then incubated at room temperature for at least an additional 1 h. For imaging, the coverslips were placed in a chamber at room temperature. Images of Fura-2-loaded cells with the excitation wavelength alternating between 340 and 380 nm were captured using a Cohu 4915 low light CCD camera on an InCyt Dual-wavelength Fluorescence Imaging and Photometry System (Intracellular Imaging Inc.). The ratio of fluorescence intensity at the two wavelengths was calculated and plotted as a function of time.

Treatment of Cells with Oligonucleotides—Phosphorothioate-modified oligonucleotides were purchased from Invitrogen. The antisense sequence used was 5'-GAC CGG AGG GGC GCT CAT-3' for PKC μ based on the start codon (ATG) plus the 15 additional downstream bases in the human PKC μ sequence. The sequences of sense and antisense were 5'-ATG AGC GCC CCT CCG GTC-3' and GCA GCA CAT CGC ATC GAC-3', respectively (15). CHO/rVR1 cells or DRG neurons were transfected with Lipofectamine 2000 as recommended by the manufacturer with minor modifications. Briefly, for CHO/rVR1 cells, 1 day before transfection, 1 \times 10⁵ cells/well were plated into 24-well plates in 0.5 ml of growth medium without antibiotics so that they were 30–50% confluent at the time of transfection. For transfection, the oligonucleotide-Lipofectamine 2000 complexes were prepared as follows (per well). 20 pmol of oligonucleotide was diluted in 50 μ l of Opti-MEM@ I reduced serum medium (Invitrogen) and gently mixed. Lipofectamine 2000 (1 μ l) was added to 50 μ l of Opti-MEM@ I medium and mixed gently. After a 5-min incubation at room temperature, the diluted oligonucleotide was combined with the diluted Lipofectamine 2000, mixed, and incubated for 20 min at room temperature to allow the oligonucleotide-Lipofectamine 2000 complexes to form. The 100 μ l of oligonucleotide-Lipofectamine 2000 complex were then added to the well and mixed gently by rocking the plate back and forth. Oligonucleotide incubation medium was replaced every 12 h for 48 h. For DRG neurons, isolated DRG neurons were seeded in 24-well plates at a density of 1 \times 10⁵ cells/well. After 24 h of culture at 37 $^{\circ}\text{C}$, the DRG neurons were transfected with oligonucleotide following the same procedure as was used for the CHO/rVR1 cells.

Subcloning of PKC μ and Mutagenesis of PKC μ and rVR1—The human PKC μ cDNA cloned in pBluescript SK(±) vector was the kind gift of Dr. K. Pfenmaier (Institute of Cell Biology and Immunology, University of Stuttgart, Germany). To generate the GFP fusion construct, PKC μ was amplified by PCR and subcloned into the XhoI-MluI site of a pEGFP-N1 vector (Clontech) modified by inserting a MluI linker into the plasmid digested with SmaI.

The kinase-inactive D727A PKC μ was prepared by mutating an aspartic acid in the 727-position to an alanine in the pEGFP-N1-PKC μ plasmid, and the GFPPrVR1S116A was prepared by mutating a serine in the 116-position to an alanine in the pEGFP-N3-rVR1 plasmid. Mu-

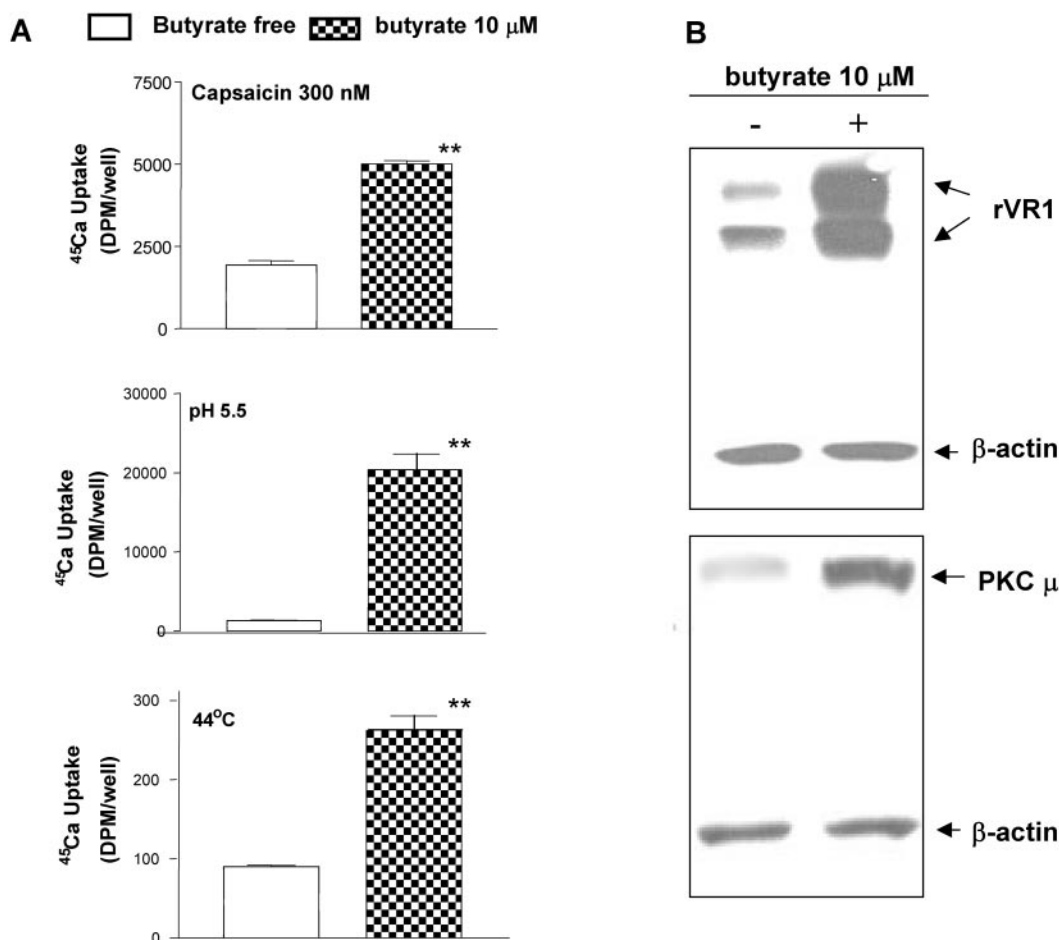


FIG. 1. Effects of butyrate on the activity of rVR1 and the expression level of rVR1 and PKC μ . A, comparison of $^{45}\text{Ca}^{2+}$ uptake induced by 300 nM capsaicin, pH (pH 5.5), and temperature (44 $^{\circ}\text{C}$) in CHO/rVR1 cells treated with or without 10 μM butyrate. The bars represent mean values of quadruplicate determinations in single, representative experiments; error bars indicate S.E. B, the expression level of rVR1 and PKC μ in CHO/rVR1 cells treated with or without 10 μM butyrate as detected by Western blot. All experiments were repeated at least two additional times with similar results. **, $p < 0.01$ as compared with butyrate free group.

tagenesis was performed with the QuikChangeTM site-directed mutagenesis kit (Stratagene, La Jolla, CA).

The mutation was confirmed by sequencing performed by the DNA minicore, Center for Cancer Research, NCI, National Institutes of Health (Bethesda, MD).

Generation of Glutathione S-Transferase (GST)-rVR1 Fusion Protein—To generate N-terminal GST-tagged rVR1 (amino acids 1–838), we have used the Gateway system (Invitrogen) following the manufacturer's protocol. rVR1 was amplified by PCR from the pEGFP-N3-rVR1 plasmid (16) and subcloned into the pDONR201 and pDEST27 vectors. The cytoplasmic N-terminal domains (amino acids 1–99, 1–118, and 1–432, respectively) and C-terminal domain (amino acids 686–838) were obtained using the same procedure. The constructs were verified by sequencing (sequence identical with AF-029310). The rat VR1-GST fusion proteins were expressed in CHO cells using Lipofectamine Plus reagent as recommended by the manufacturer (Invitrogen). 48 h after transfection, the cells were washed three times with cold DPBS (Ca^{2+} - and Mg^{2+} -free), harvested in PBS with proteinase inhibitor (proteinase inhibitor tablet from Roche Applied Science), sonicated, and added to the same volume of detergent mixture (50 mM Tris-HCl, pH 7.5, 150 mM NaCl, 1% Triton X-100, 1% Nonidet P-40, 0.5% deoxycholate with proteinase inhibitor and 2% (v/v) β -mercaptoethanol). The mixture was rotated at 4 $^{\circ}\text{C}$ for 2–3 h and centrifuged for 20 min at 15,000 rpm, and the supernatant was added to glutathione-SepharoseTM 4 Fast Flow beads (Amersham Biosciences). After being rotated overnight at 4 $^{\circ}\text{C}$, the beads were washed twice with 2 \times diluted detergent mixture (same as above) containing β -mercaptoethanol and then washed twice with PBS containing β -mercaptoethanol (0.1%, v/v). The fusion protein was eluted with 10 mM reduced glutathione. The purity of the protein was determined by SDS-polyacrylamide gel electrophoresis and staining with Coomassie Brilliant Blue.

Western Blotting—Cells were harvested and lysed in a buffer con-

taining 50 mM Tris-HCl, pH 7.4, 150 mM NaCl, 1.5 mM MgCl_2 , 10% glycerol, 1% Triton X-100, 5 mM EGTA, 20 μM leupeptin, 1 mM phenylmethylsulfonyl fluoride, 1 mM NaVO_3 , 10 mM NaF, and proteinase inhibitor mixture. Equal amounts of protein (20 μg) were subjected to SDS-PAGE and electrotransferred to nitrocellulose membranes. Membranes were blocked with 5% nonfat milk, 2% bovine serum albumin, and 5% normal goat serum in Tris-buffered saline (TBS) for 1 h at room temperature. Membranes were then probed with a primary antibody against the specific protein, washed four times with 0.2% Tween 20 in TBS, and then subjected to a second incubation with anti-mouse or anti-rabbit secondary antibody conjugated to horseradish peroxidase (1:1000; Bio-Rad). Bands were visualized by the ECL Western blotting detection system (Amersham Biosciences). The primary antibodies were polyclonal anti-capsaicin receptor antibody (1:100; Calbiochem), a polyclonal anti-PKC μ (C-20) antibody (1:1000; Santa Cruz Biotechnology), a monoclonal anti-GFP antibody (1:1000; Roche Applied Science), and a monoclonal anti-GST antibody (1:1000; Amersham Biosciences).

In Vitro Binding—GST fusion proteins immobilized on glutathione-Sepharose beads were incubated with 1 μg of recombinant PKC μ (Calbiochem) in TBS buffer with 0.1% Triton X-100 for 5 h at 4 $^{\circ}\text{C}$. Beads were washed three times with incubation buffer, and bound proteins were eluted in 30 μl of SDS-PAGE sample buffer and processed for 4–20% Tricine SDS-polyacrylamide gradient gel electrophoresis. Separated proteins were transferred and detected sequentially using a polyclonal anti-PKC μ antibody and a monoclonal anti-GST antibody on the same blot. Horseradish peroxidase-conjugated secondary antibodies and ECL (Amersham Biosciences) were used to visualize bands.

Co-immunoprecipitation between rVR1 and PKC μ in the rVR1 Heterologous Expression System—GFP-rVR1 and GFP empty vector were transfected into CHO cells individually using Lipofectamine Plus reagent (Invitrogen). 48 h after transfection, cells were washed three times with cold PBS and then lysed with 500 μl of lysis buffer containing 50

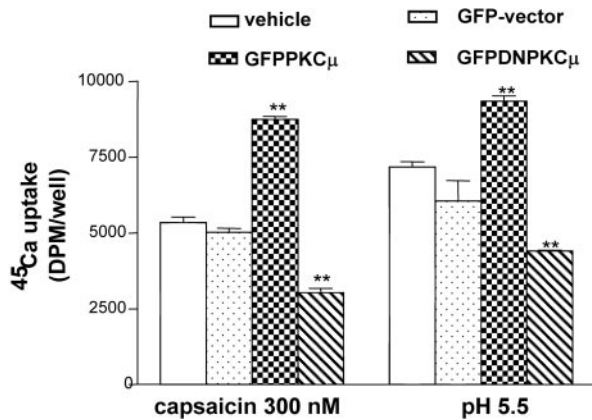


FIG. 2. Effects of overexpression of PKC μ and dominant negative PKC μ on the activity of rVR1 as determined by ⁴⁵Ca²⁺ uptake. CHO/rVR1 cells were transfected with GFPPCK μ and dominant negative GFPPCK μ (GFPDNPCK μ) for 48 h. The response of CHO/rVR1 cells to 300 nM capsaicin or low pH (pH 5.5) was detected by ⁴⁵Ca²⁺ uptake. Overexpression of GFP empty vector and mock transfection with vehicle alone were used as control. Bars, mean values of quadruplicate determinations in single, representative experiments; error bars, S.E. All experiments were repeated at least two additional times with similar results. **, $p < 0.01$ as compared with vehicle group.

mm Tris-HCl, pH 7.4, 150 mM NaCl, 1.5 mM MgCl₂, 10% glycerol, 1% Triton X-100, 5 mM EGTA, 20 μ M leupeptin, 1 mM phenylmethylsulfonyl fluoride, 1 mM NaVO₃, 10 mM NaF, and proteinase inhibitor mixture. The lysates were centrifuged at 12,000 rpm at 4 °C for 15 min to remove cellular debris. The supernatant was incubated with either 5 μ l of anti-GFP (1:100) monoclonal antibody, or mouse control IGG at 4 °C for 1 h. Protein A-Sepharose CL-4B resin (Santa Cruz Biotechnology, Inc., Santa Cruz, CA) was added to the samples, and the incubation was continued for a further 3 h, after which samples were washed three times with TBS, 0.1% Triton X-100. Separated proteins were transferred and detected sequentially using a polyclonal anti-PKC μ antibody and a monoclonal anti-GST antibody on the same blot. Horseradish peroxidase-conjugated secondary antibodies and ECL (Amersham Biosciences) were used to visualize bands. For multiple detection with different antibodies, blots were first stripped in a solution of 62.5 mM Tris-HCl, pH 7.5, 20 mM dithiothreitol, and 1% SDS for 20–30 min at 50 °C and washed twice for 15 min with TBS, 0.1% Tween 20, followed by blocking and incubation with a new primary antibody.

Co-immunoprecipitation between rVR1 and PKC μ in the Endogenous DRG System—2–3-Week-old rats were killed by decapitation under CO₂ anesthesia. The spinal columns were removed aseptically, and dorsal root ganglia from all levels were dissected out and homogenized in lysis buffer as above. After being rotated at 4 °C for 1 h, the lysates were centrifuged at 12,000 rpm at 4 °C for 15 min to remove cellular debris. The supernatant was incubated with either 5 μ l of anti-PKC μ (1:100) polyclonal antibody or rabbit control IGG at 4 °C for 12 h. Protein A-Sepharose CL-4B resin (Santa Cruz Biotechnology) was added to the samples and the incubation was continued for a further 12 h, after which samples were washed six times with TBS, 0.1% Triton X-100. The subsequent steps were similar to those with the heterologous rVR1 system.

Phosphorylation Reactions—Phosphorylation by PKC μ of rVR1 and different N-terminal fragments was assessed following immunoprecipitation. Cultured CHO cells were treated with 100 nM PMA or control solvent (Me₂SO; 0.1% (v/v) final concentration) for 20 min and then washed three times with ice-cold PBS and lysed in 500 μ l of lysis buffer. PKC μ was immunoprecipitated from cell lysates with PKC μ (C-20) antibody (1:100) at 4 °C for 3 h. Immune complexes were recovered by the addition of 50 μ l of Protein A-Sepharose (1 mg/ml; Santa Cruz Biotechnology), and pellets were washed three times with lysis buffer and three times with assay buffer (30 mM Tris-HCl (pH 7.5), 10 mM MgCl₂, and 1 mM dithiothreitol). The final pellet was resuspended in assay buffer to yield a total volume of 40 μ l. To initiate the phosphorylation reaction, 10 μ l of phosphorylation mix (assay buffer containing GSTrVR1 or the GSTrVR1 N-terminal fragments or GST alone (10 μ g/ml) and 5 μ Ci of [γ -³²P]ATP) was added. The mixture was incubated at 30 °C for 20 min, and the reaction was terminated by the addition of SDS-PAGE sample buffer. After boiling for 5 min,

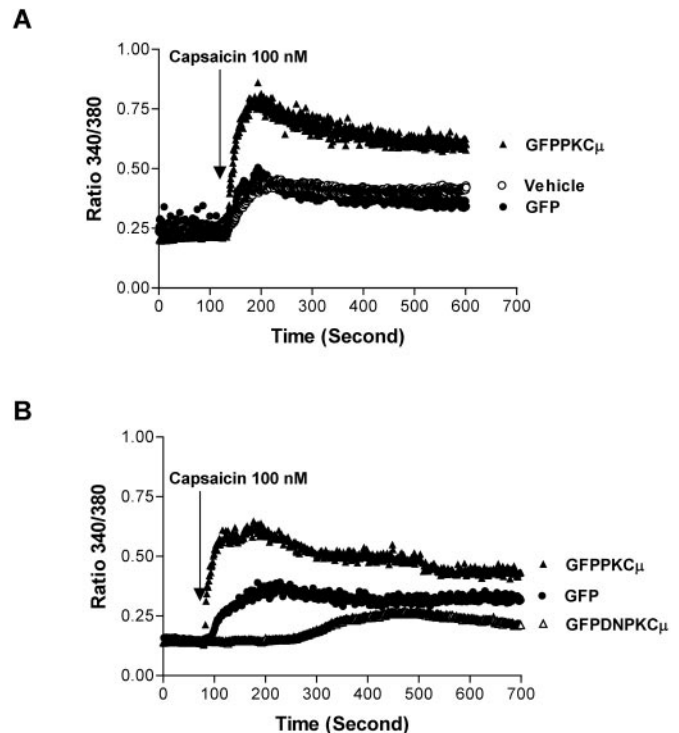


FIG. 3. Effects of overexpression of PKC μ and dominant negative PKC μ on the activity of rVR1 as determined by calcium imaging. A, CHO/rVR1 cells were transfected with GFPPCK μ or GFP for 48 h; the response of CHO/rVR1 cells to 100 nM capsaicin was detected by calcium imaging. B, CHO/rVR1 cells were transfected with GFPPCK μ , GFP, or dominant negative GFPPCK μ (GFPDNPCK μ) for 48 h. The response of CHO/rVR1 cells to 100 nM capsaicin was detected by calcium imaging. Overexpression of GFP empty vector and mock transfection with vehicle alone were used as controls. Points represent the averaged signal from a minimum of 16 cells imaged simultaneously. The arrows indicate the start of the treatment. Each experiment was repeated at least an additional two times with similar results on independently cultured cells.

the samples were subjected to SDS-PAGE. The gels were stained with Coomassie Brilliant Blue, dried, and exposed to x-ray film for autoradiography.

Visualization by Confocal Microscopy of GFPPCK μ Translocation—Prior to observation, CHO/rVR1 cells were cultured on 40-mm round coverslips in the culture medium with tetracycline (1 μ g/ml) and Geneticin (0.25 mg/ml). 24 h later, GFPPCK μ was transiently transfected into the cells with Lipofectamine Plus reagent as recommended by the manufacturer (Invitrogen). After a 4-h incubation with the DNA and Lipofectamine complex, the medium was replaced with CHO/rVR1-inducing culture medium with Geneticin (0.25 mg/ml) without tetracycline at 35 or 37 °C for a further 48 h. Before the measurement, the coverslips were introduced into the microscope chamber system, which was connected to a temperature controller set to 37 °C, and medium was perfused through the chamber with a model P720 microperfusion pump (Instech, Plymouth Meeting, PA). The images of the cells were collected at 1-min intervals using LaserSharp software through a Bio-Rad MRC 1024 confocal scan head mounted on a Nikon Optiphot microscope with a 60 \times planapochromat lens. A krypton-argon gas laser provided excitation at 488 nm with a 522/32 emission filter for green fluorescence.

RESULTS

Butyrate, a Histone Deacetylase Inhibitor, Enhanced the Activity of rVR1 and PKC μ Expression—Sodium butyrate is a histone deacetylase inhibitor. Histone acetylation influences the higher order structure of chromatin, resulting in a chromatin conformation that is more accessible to transcription factors and leading to enhanced transcription of some genes (17). As part of our effort to optimize conditions for evaluating VR1 pharmacology, we have found that butyrate can influence the function of VR1. Expression of rVR1 was induced in CHO/rVR1

FIG. 4. Effects of PKC μ antisense oligonucleotide on the activity of rVR1 in CHO/rVR1 cells. *A*, CHO/rVR1 cells were treated with PKC μ antisense oligonucleotides for 48 h; the response of CHO/rVR1 cells to 100 nM capsaicin was determined by $^{45}\text{Ca}^{2+}$ uptake. Treatments with vehicle or PKC μ sense or missense oligonucleotides were used as controls. *Bars*, mean values of quadruplicate determinations in single, representative experiments; *error bars*, S.E. Each experiment was repeated at least an additional two times with similar results on independently cultured cells. *B*, the expression level of PKC μ in CHO/rVR1 cells treated with antisense, sense, or missense as determined by Western blot. Each experiment was repeated at least an additional two times with similar results on independently cultured cells. **, $p < 0.01$ as compared with the sense group; ##, $p < 0.01$ as compared with the missense group.

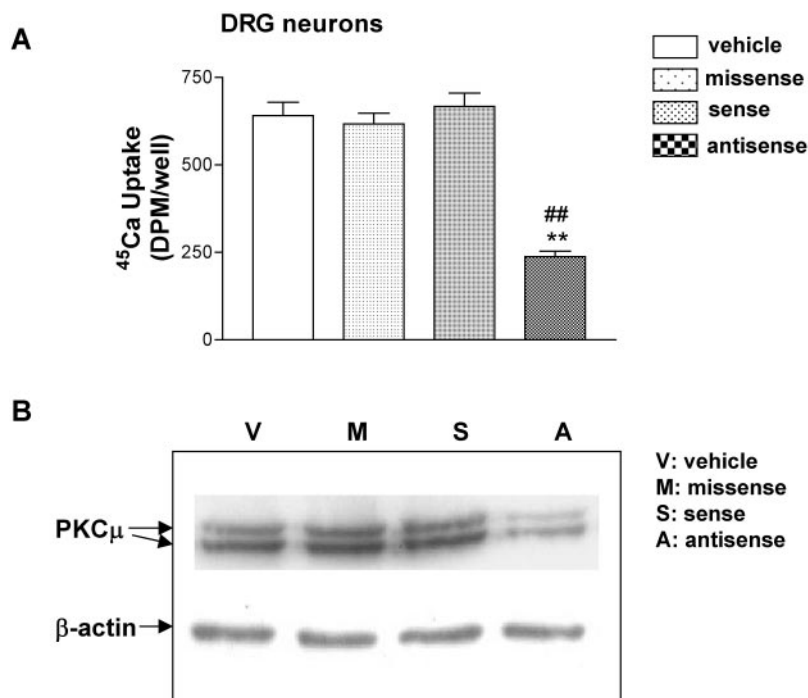
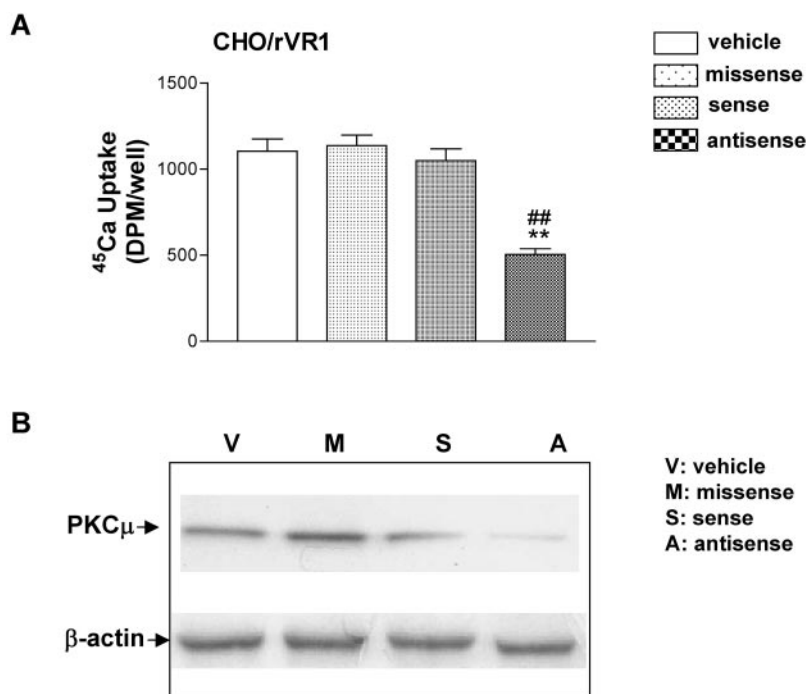


FIG. 5. Effects of PKC μ antisense oligonucleotides on the activity of rVR1 in primary cultured DRG neurons. *A*, DRG neurons were treated with PKC μ antisense oligonucleotides for 48 h; the response of DRG neurons to 100 nM capsaicin was determined by $^{45}\text{Ca}^{2+}$ uptake. *Bars*, mean values of quadruplicate determinations in single, representative experiments; *error bars*, S.E. *B*, the expression level of PKC μ in DRG neurons treated with antisense, sense, or missense as determined by Western blot. Each experiment was repeated at least an additional two times with similar results on independently cultured cells. **, $p < 0.01$ as compared with the sense group; ##, $p < 0.01$ as compared with the missense group.

cells by a change of medium to medium without tetracycline either in the presence or absence of sodium butyrate (10 μM). The butyrate dramatically enhanced the functional activity of rVR1 as evidenced by increased uptake of $^{45}\text{Ca}^{2+}$ in response to capsaicin, low pH (pH 5.5), and high temperature (44 $^{\circ}\text{C}$) (Fig. 1A). Likewise, the level of expression of rVR1 increased, as did that of PKC μ (Fig. 1B) and PKC β 1 (data not shown); the level of expression of other PKC isoforms was not changed. Because of the reported effects of PKA and several PKC isoforms on rVR1 activity (3, 4, 19), these observations suggested that the increased activity of rVR1 in response to butyrate might reflect not only the enhanced expression of the rVR1 protein itself but also an effect of the elevated PKC μ and/or PKC β 1 on the activity of rVR1.

Overexpression of PKC μ in CHO/rVR1 Cells Enhanced the Activity of rVR1, and Expression of a Dominant Negative PKC μ Mutant Attenuated the Activity of rVR1—To investigate the possible role of PKC μ on the activity of rVR1, we overexpressed GFPPKC μ in CHO/rVR1 cells. Overexpression of PKC μ enhanced the uptake of $^{45}\text{Ca}^{2+}$ in response to capsaicin (300 nM) and low pH (pH 5.5) (Fig. 2). Conversely, when we expressed a kinase-negative mutant of PKC μ , which would be expected to function as a dominant negative, the dominant negative GFP-PKC μ attenuated the response of rVR1 as detected by $^{45}\text{Ca}^{2+}$ uptake (Fig. 2), arguing that the endogenous PKC μ influenced rVR1 function. We further evaluated the effects of overexpression of PKC μ or expression of the dominant negative PKC μ by calcium imaging. As observed for $^{45}\text{Ca}^{2+}$ uptake, PKC μ over-

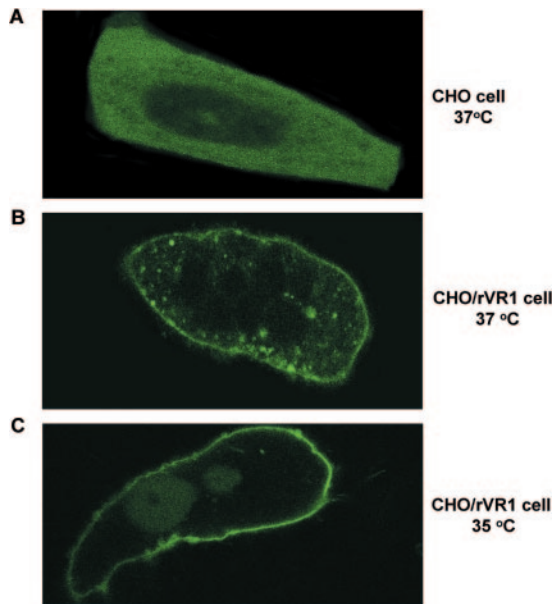


FIG. 6. The localization of GFP μ PKC in CHO/rVR1 and CHO cells visualized by confocal microscopy. A, CHO cells were transfected with GFP μ PKC and cultured at 37 °C for 48 h. B, CHO/rVR1 cells were transfected with GFP μ PKC and were then induced for VR1 expression by culturing in the absence of tetracycline at 37 °C for 48 h. C, CHO/rVR1 cells were transfected with GFP μ PKC and were then induced for VR1 expression by culturing in the absence of tetracycline at 35 °C for 48 h. Localization of GFP μ PKC was visualized by confocal microscopy. Each experiment was repeated at least an additional two times with similar results on independently cultured cells.

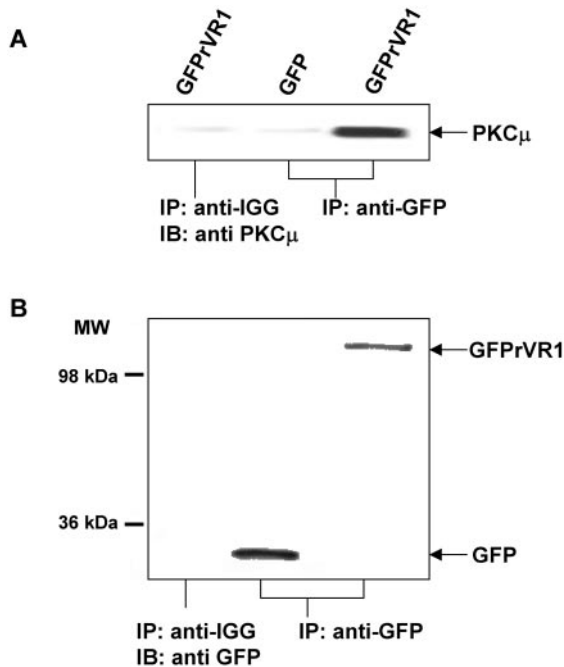


FIG. 7. Co-immunoprecipitation of GFP μ rVR1 with PKC μ in CHO cells. CHO cells were transfected with GFP empty vector or GFP μ rVR1. After 48 h, the supernatants of cell lysates were immunoprecipitated (IP) with anti-GFP antibody or IGG and collected by Protein A-Sepharose CL-4B resin; the immunocomplex was analyzed by SDS-PAGE and sequential immunoblotting (IB) with anti-PKC μ antibody (A) and anti-GFP antibody (B). Each experiment was repeated at least an additional two times with similar results on independently cultured cells.

expression enhanced the elevation in internal calcium in response to capsaicin, and the dominant negative mutant diminished the response (Fig. 3, A and B).

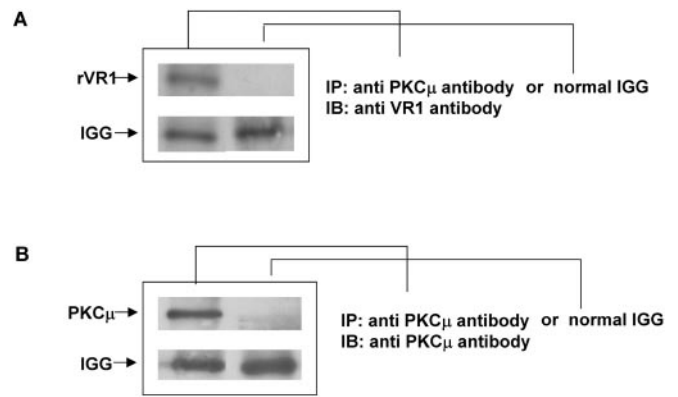


FIG. 8. Co-immunoprecipitation of endogenous rVR1 with PKC μ in DRG neurons. The supernatants of rat DRG lysates were immunoprecipitated (IP) with anti-PKC μ antibody or normal IGG as control and collected by Protein A-Sepharose CL-4B resin; the immunocomplex was analyzed by SDS-PAGE and sequential immunoblotting (IB) with anti-VR1 antibody (A) and anti-PKC μ antibody (B). Each experiment was repeated at least an additional two times with similar results on independent samples.

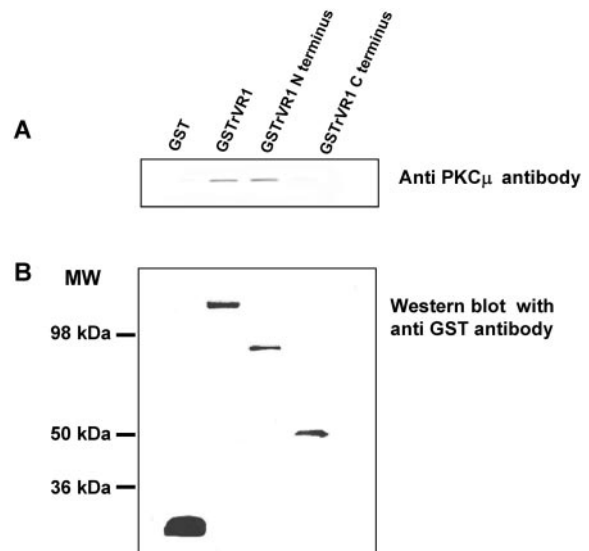


FIG. 9. PKC μ bound directly to full-length rVR1 and the rVR1 N-terminal fragment *in vitro*. GST fusion proteins immobilized on glutathione-Sepharose beads were incubated with recombinant PKC μ . Bound proteins were eluted in SDS-PAGE sample buffer and processed for 4–20% Tricine SDS-polyacrylamide gradient gel electrophoresis. Separated proteins were sequentially detected using a polyclonal anti-PKC μ antibody (A) and a monoclonal anti-GST antibody on the same blot (B). Each experiment was repeated at least an additional two times with similar results on independently cultured cells.

Pretreatment of PKC μ Antisense on CHO/rVR1 Cells or Primary Cultured DRG Neurons Inhibited the Response Induced by Capsaicin—To further assess the effect of endogenous PKC μ on VR1, we used antisense oligonucleotide to decrease endogenous PKC μ expression in CHO/rVR1 cells and then evaluated the response of the cells to capsaicin (100 nM). Immunoblot analysis confirmed that PKC μ expression was partially blocked upon treatment with the specific antisense oligonucleotide (Fig. 4B); a little inhibition was observed upon treatment with sense oligonucleotide, and no significant change occurred upon treatment with missense oligonucleotide as compared with the group treated with transfection reagents without oligonucleotide. Functionally, preincubation of cells with specific antisense for 48 h resulted in a 51.9 ± 6.7% and a 55.5 ± 8.2% decrease in ⁴⁵Ca²⁺ uptake in response to capsaicin as compared with the control groups of sense and missense oligonucleotide treat-

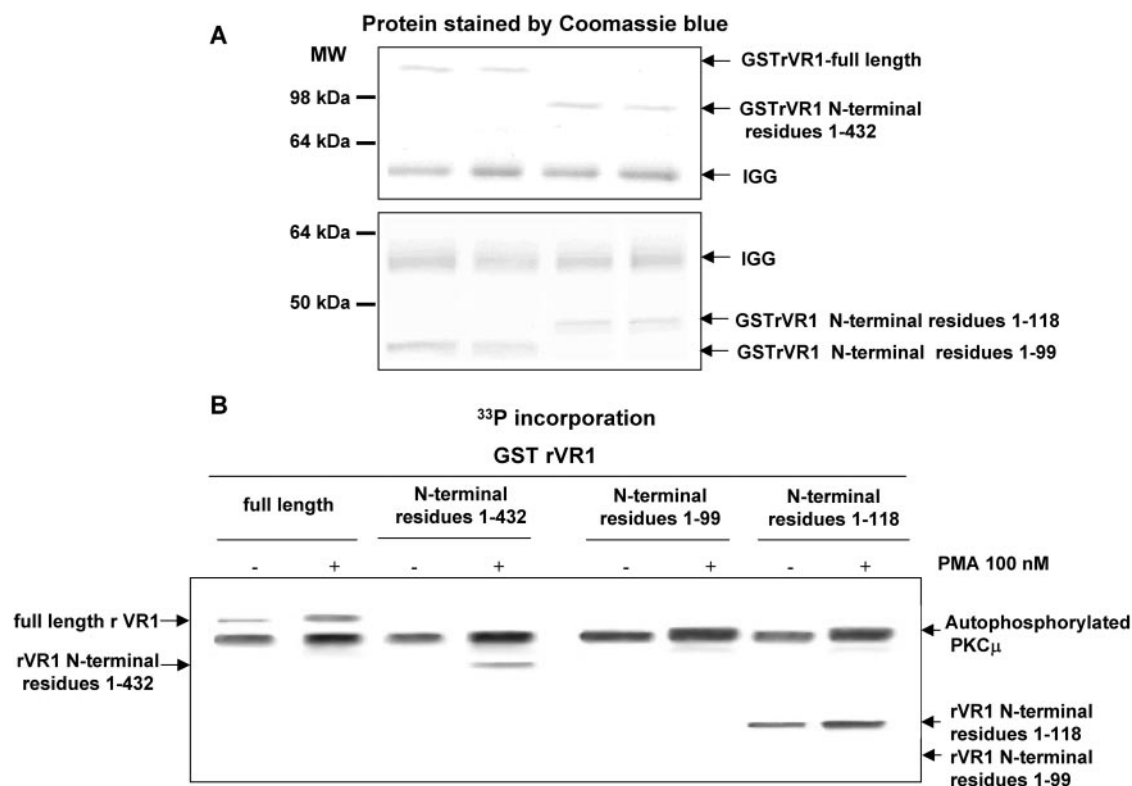


FIG. 10. Phosphorylation by PKC μ of full-length rVR1 and different N-terminal fragments of rVR1. Cultured CHO cells were treated with 100 nM PMA or control vehicle (Me₂SO; final concentration 0.1% (v/v)) for 20 min. Cell lysates were prepared, and PKC μ was immunoprecipitated with anti-PKC μ (C-20) antibody (1:100). Immune complexes were recovered by protein A-Sepharose, washed, and resuspended in phosphorylation assay buffer. To initiate the phosphorylation reaction, 10 μ l of phosphorylation mix (assay buffer containing GSTrVR1 or the fusion protein between GST and the different N-terminal fragments or GST (10 μ g/ml) and 5 μ Ci of [γ -³²P]ATP) was added. The mixture was incubated at 30 °C for 20 min, and the reaction was terminated by the addition of SDS-PAGE sample buffer. After boiling for 5 min, the samples were subjected to SDS-PAGE. Gels were then stained with Coomassie Blue (A), dried, and exposed to x-ray films for autoradiography (B). Each experiment was repeated at least an additional two times with similar results on independently cultured cells.

ment, respectively. There was no detectable effect following treatment with the sense or missense oligonucleotides as compared with treatment with transfection reagents without oligonucleotide (Fig. 4A).

To verify that the behavior of PKC μ as a modulator of rVR1 was not an artifact of the CHO/rVR1 heterologous expression system, we also examined the effect of treatment of cultured rat DRG neurons with the antisense oligonucleotide. As observed in the case of the CHO/rVR1 cells, antisense treatment was able to markedly reduce the level of PKC μ in DRG neurons compared with controls treated with sense or missense oligonucleotides (Fig. 5B). Likewise, ⁴⁵Ca²⁺ uptake by the cultured DRG neurons in response to 100 nM capsaicin was significantly reduced by treatment with the antisense oligonucleotide compared with control, sense, or missense oligonucleotide-treated cells (Fig. 5B).

GFPPKC μ Was Localized to the Cytoplasmic Membrane of CHO/rVR1 Cells but Not of CHO Cells—To further understand the interaction between PKC μ and rVR1, we examined the localization of PKC μ in the cells. GFPPKC μ was transfected into CHO/rVR1 cells, which were then induced for rVR1 expression by culturing in the absence of tetracycline at 37 °C for 48 h. Under these conditions, the GFPPKC μ localized to the cytoplasmic membrane of the CHO/rVR1 cells (Fig. 6B). Interestingly, in the CHO cells without rVR1, GFPPKC μ localized predominantly to the cytoplasm (Fig. 6A). Since VR1 is a non-selective cation channel and sensitive to high temperature, in order to exclude a nonspecific effect of temperature, the CHO/rVR1 cells transfected with GFPPKC μ were incubated at a lower temperature, 35 °C, for comparison. Under these conditions, likewise, GFPPKC μ localized to the cytoplasmic membrane of the CHO/rVR1 cells (Fig. 6C). These results argue that

the presence of rVR1 influenced PKC μ localization, whether directly or indirectly.

Direct Interaction between PKC μ and rVR1—The modulation of the activity of rVR1 by PKC μ could be either direct or indirect. Consistent with a direct interaction between rVR1 and PKC μ , in CHO cells expressing GFPPrVR1, immunoprecipitation of the rVR1 with monoclonal anti-GFP antibody co-immunoprecipitated endogenous PKC μ (Fig. 7). Only background levels of PKC μ were immunoprecipitated in the CHO cells expressing GFPPrVR1 when control IGG was used or in CHO cells expressing GFP alone upon immunoprecipitation with monoclonal anti-GFP antibody.

A similar result was obtained using rat DRGs and antibodies directed against rVR1 and PKC μ . We conclude that the interaction thus occurs at the endogenous levels of rVR1 and PKC μ expression in the physiologically relevant context of the DRG neuron; it is not simply an artifact of an engineered system (Fig. 8).

In vitro binding experiments were performed to confirm the direct interaction of PKC μ and rVR1. Fusion proteins between GST and the full-length rVR1 or the N or C termini of rVR1 were immobilized on glutathione-Sepharose beads and incubated with recombinant PKC μ ; the bound proteins were then analyzed by Western blotting. Both the full-length rVR1 and the N terminus of rVR1 bound PKC μ , whereas the C-terminal portion of rVR1 or GST alone did not (Fig. 9A). Controls confirmed (Fig. 9B) that similar amounts of the GST-full-length rVR1, GSTrVR1 N-terminal fragment, and GSTrVR1 C-terminal fragment bound to the beads. These experiments suggest that PKC μ and rVR1 interact directly and that the interaction depends on the presence of the N-terminal portion of rVR1.

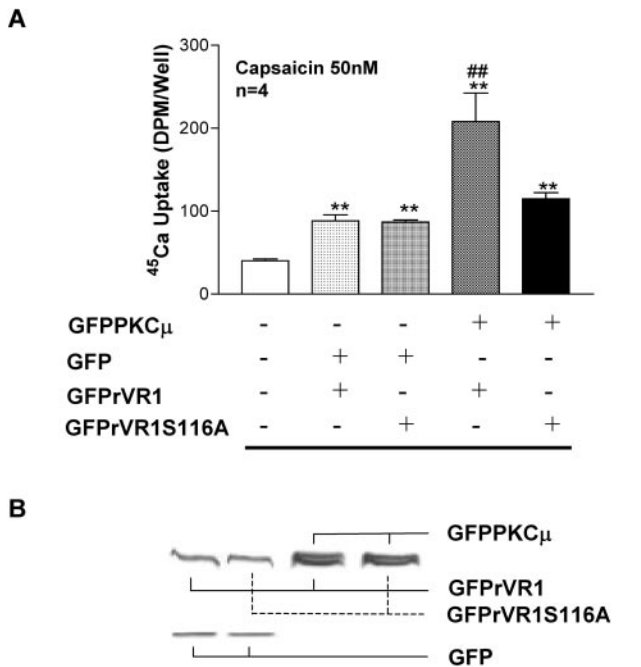


FIG. 11. Effect of overexpression of PKC μ on the activity of wild type rVR1 and the rVR1S116A mutant as determined by $^{45}\text{Ca}^{2+}$ uptake. A, wild type GFPPrVR1 or GFPPrVR1S116A was co-transfected with GFPPKC μ into CHO cells, and incubation continued for 48 h. The response of the cells to 50 nM capsaicin was determined by $^{45}\text{Ca}^{2+}$ uptake. Co-expression with GFP empty vector and mock transfection with vehicle alone were used as controls. Bars, mean values of quadruplicate determinations in single, representative experiments; error bars, S.E. B, the expression level of GFP, wild type GFPPrVR1, GFPPrVR1S116A, and GFPPKC μ were determined by Western blot using anti-GFP antibody. Each experiment was repeated at least an additional two times with similar results on independently cultured cells. **, $p < 0.01$ as compared with the no treatment group. ##, $p < 0.01$ as compared with the GFPPrVR1S116A plus GFPPKC μ group.

PKC μ Directly Phosphorylated Full-length rVR1 and N-terminal Fragments of rVR1—Since PKC μ bound directly to rVR1 and its full-length N-terminal fragment, we asked whether PKC μ could directly phosphorylate VR1 and its N-terminal fragment. PKD/PKC μ is activated by phosphorylation through a PKC-dependent pathway in all systems examined *in vivo* (7). The increased activity of phosphorylated PKD is maintained during cell disruption and immunoprecipitation. We therefore used activated, immunoprecipitated PKC μ to evaluate rVR1 phosphorylation. PKC μ was incubated with GSTrVR1, with the GSTrVR1 N-terminal fragment (residues 1–432) and with the shorter GST-N-terminal fragments (residues 1–118 and residues 1–99). We found that PKC μ was able to directly phosphorylate full-length rVR1, the full-length N-terminal fragment of rVR1 (residues 1–432), and the N-terminal fragment comprising the first 118 amino acids of rVR1 (Fig. 10B). It did not, however, phosphorylate the N-terminal fragment comprising the first 99 amino acids, suggesting a possible phosphorylation site of PKC μ between amino acids 99 and 118. A candidate phosphorylation site for PKC μ in this region is serine 116.

Identification of Serine 116 of rVR1 as the Phosphorylation Site for PKC μ —To confirm whether serine 116 indeed is a site of regulation by PKC μ , wild type GFPPrVR1 or a GFPPrVR1S116A mutant was cotransfected with GFPPKC μ into CHO cells, and then the response of the cells to capsaicin was evaluated by $^{45}\text{Ca}^{2+}$ uptake. For comparison, the effect of the co-transfection with GFPPKC μ was compared with that with GFP. Overexpression of GFPPKC μ increased the response to capsaicin of wild type GFPPrVR1 but not of the

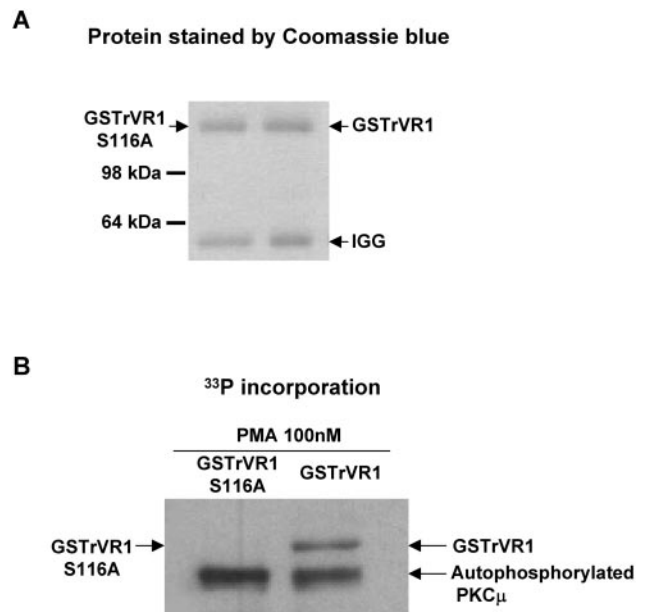


FIG. 12. PKC μ could not phosphorylate GSTrVR1S116A. Cultured CHO cells were treated with 100 nM PMA or control vehicle (Me_2SO ; final concentration 0.1% (v/v)) for 20 min. Cell lysates were prepared, and PKC μ was immunoprecipitated with anti-PKC μ (C-20) antibody (1:100). Immune complexes were recovered by protein A-Sepharose, washed, and resuspended in phosphorylation assay buffer. To initiate the phosphorylation reaction, 10 μl of phosphorylation mix (assay buffer containing GSTrVR1 or GSTrVR1S116A (10 $\mu\text{g}/\text{ml}$) and 5 μCi of [$\gamma\text{-}^{33}\text{P}$]ATP) was added. The mixture was incubated at 30 $^\circ\text{C}$ for 20 min, and the reaction was terminated by the addition of SDS-PAGE sample buffer. After boiling for 5 min, the samples were subjected to SDS-PAGE. Gels were then stained with Coomassie Blue (A), dried, and exposed to x-ray films for autoradiography (B). Each experiment was repeated at least an additional two times with similar results on independently cultured cells.

GFPPrVR1S116A mutant ($p < 0.01$ as compared with the GFPPrVR1S116A plus GFPPKC μ group) (Fig. 11A). In addition, we also confirmed that PKC μ phosphorylated GSTrVR1 but not GSTrVR1S116A (Fig. 12). We conclude that serine 116 of rVR1 indeed is a functional target for PKC μ .

DISCUSSION

Our findings that PKC μ binds to, phosphorylates, and influences VR1 activity in response to capsaicin, heat, and pH further emphasize the multiplicity of signaling pathways that impact VR1 function. These pathways provide potential points of intervention in the treatment of conditions involving VR1 function. The identification of PKC μ in particular further emphasizes the complex nature of VR1 regulation. PKC ϵ has already been implicated in the development of thermal hyperalgesia, as evidenced by a blunted response in mice in which PKC ϵ has been knocked out (18). Furthermore, PKC ϵ has been shown to directly phosphorylate VR1, providing a plausible direct mechanism for the effect of PKC ϵ (19). It is known, however, that PKC ϵ also phosphorylates and thereby activates PKC μ (20). A second possible pathway for the PKC ϵ effects on VR1 is therefore indirect, via PKC μ . Because PKC μ has a very different kinase domain from the PKCs, as already discussed, PKC μ provides a novel and distinct target for kinase inhibitors targeted to influence VR1 function.

Our findings also have an important impact for understanding the function of PKC μ . A growing number of proteins, such as phosphatidylinositol kinases (9), 14-3-3 proteins (10), B-cell receptor complexes (11), the tyrosine kinase Syk (12), phospholipase C γ 1 (11), Btk (8), and the two novel PKCs PKC ϵ and PKC η directly interact with PKC μ (21), but none of these

interacting proteins has been shown to be a PKC μ substrate. An exception is Kidins220, which was isolated from PC12 cells, interacts with PKD, and is directly phosphorylated by PKD (13). Structural comparison of Kidins220 and VR1 reveals similarities. Both are integral membrane proteins with N-terminal segments of similar length containing ankyrin repeats and with both the N-terminal and C-terminal domains in the cytoplasm. Our deletion results suggest a phosphorylation site in the N-terminal domain of rVR1 between amino acids 99 and 118. PKC μ /PKD prefers peptide substrates with basic residues upstream of the phosphorylation site serine, a hydrophobic amino acid (Phe, Leu, or Val) at the +1-position, and a critical Leu residue at the -5-position (22). Ser¹¹⁶ (sequence LY-DRRSIF) represents such a consensus sequence. Finally, we showed by site-directed mutagenesis that mutation of this residue S116A blocks both the phosphorylation of rVR1 by PKC μ and the enhancement by PKC μ of the response of rVR1 to capsaicin (Figs. 11 and 12). Ser¹¹⁶ is also a major phosphorylation site in VR1 for PKA, and this site has been shown to be involved in VR1 desensitization (3). Our results thus suggest that PKC μ should likewise influence desensitization, with the relative importance of PKA and PKC μ depending on the relative activity of these two pathways in a specific system. Our results using the antisense construct to PKC μ in the rat DRG neuronal cells suggest that the PKC μ pathway may have physiological importance in these cells.

Histone deacetylase inhibitors are attracting interest as potential therapeutics (23). Our findings imply that their possible effects on C-fiber function through modulation of PKC μ expression should be carefully evaluated.

In this work, we identified PKC μ /PKD, a serine/threonine kinase family member, as a modulator of vanilloid receptor activity, directly associating with and phosphorylating it. Since PKC μ regulates the response of VR1 to capsaicin and low pH, it raised the possibility that VR1 may act as a PKC μ substrate

during inflammatory pain states and that PKC μ may be involved in the development of chronic pain.

REFERENCES

1. Julius, D., and Basbaum, A. I. (2001) *Nature* **413**, 203–210
2. Di Marzo, V., Blumberg, P. M., and Szallasi, A. (2002) *Curr. Opin. Neurobiol.* **12**, 372–379
3. Bhave, G., Zhu, W., Wang, H., Brasier, D. J., Oxford, G. S., and Gereau, R. W., IV (2002) *Neuron* **35**, 721–731
4. Olah, Z., Karai, L., and Iadarola, M. J. (2002) *J. Biol. Chem.* **277**, 35752–35759
5. Ji, R. R., Samad, T. A., Jin, S. X., Schmall, R., and Woolf, C. J. (2002) *Neuron* **36**, 57–68
6. Rozengurt, E., Sinnett-Smith, J., Van Lint, J., and Valverde, A. M. (1995) *Mutat. Res.* **333**, 153–160
7. Zugaza, J. L., Sinnett-Smith, J., Van Lint, J., and Rozengurt, E. (1996) *EMBO J.* **15**, 6220–6230
8. Johannes, F. J., Hausser, A., Storz, P., Truckenmuller, L., Link, G., Kawakami, T., and Pfizenmaier, K. (1999) *FEBS Lett.* **461**, 68–72
9. Nishikawa, K., Toker, A., Wong, K., Marignani, P. A., Johannes, F. J., and Cantley, L. C. (1998) *J. Biol. Chem.* **273**, 23126–23133
10. Hausser, A., Storz, P., Link, G., Stoll, H., Liu, Y. C., Altman, A., Pfizenmaier, K., and Johannes, F. J. (1999) *J. Biol. Chem.* **274**, 9258–9264
11. Sidorenko, S. P., Law, C. L., Klaus, S. J., Chandran, K. A., Takata, M., Kurosaki, T., and Clark, E. A. (1996) *Immunity* **5**, 353–363
12. Zhang, J., Berenstein, E., and Siraganian, R. P. (2002) *Mol. Cell. Biol.* **22**, 8144–8154
13. Iglesias, T., Cabrera-Poch, N., Mitchell, M. P., Naven, T. J., Rozengurt, E., and Schiavo, G. (2000) *J. Biol. Chem.* **275**, 40048–40056
14. Szallasi, A., Blumberg, P. M., Annicelli, L. L., Krause, J. E., and Cortright, D. N. (1999) *Mol. Pharmacol.* **56**, 581–587
15. Chandrasekher, G., Bazan, N. G., and Bazan, H. E. (1998) *Exp. Eye Res.* **67**, 603–610
16. Olah, Z., Szabo, T., Karai, L., Hough, C., Fields, R. D., Caudle, R. M., Blumberg, P. M., and Iadarola, M. J. (2001) *J. Biol. Chem.* **276**, 11021–11030
17. Arts, J., Lansink, M., Grimbergen, J., Toet, K. H., and Kooistra, T. (1995) *Biochem. J.* **310**, 171–176
18. Khasar, S. G., Lin, Y. H., Martin, A., Dadgar, J., McMahon, T., Wang, D., Hundle, B., Aley, K. O., Isenberg, W., McCarter, G., Green, P. G., Hodge, C. W., Levine, J. D., and Messing, R. O. (1999) *Neuron* **24**, 253–260
19. Numazaki, M., Tominaga, T., Toyooka, H., and Tominaga, M. (2002) *J. Biol. Chem.* **277**, 13375–13378
20. Waldron, R. T., and Rozengurt, E. (2003) *J. Biol. Chem.* **278**, 154–163
21. Waldron, R. T., Rey, O., Iglesias, T., Tugal, T., Cantrell, D., and Rozengurt, E. (2001) *J. Biol. Chem.* **276**, 32606–32615
22. Nishikawa, K., Toker, A., Johannes, F. J., Songyang, Z., and Cantley, L. C. (1997) *J. Biol. Chem.* **272**, 952–960
23. Chen, J. S., Faller, D.V., and Spanjaard, R. A. (2003) *Curr. Cancer Drug Targets* **3**, 219–236